Molecular Crystals and Liquid Crystals Science and Technology. Section A. Molecular Crystals and Liquid Crystals

Publication details, including instructions for authors and subscription information:
http://www.tandfonline.com/loi/gmcl19

Numerical Simulation of Nematic Liquid Crystalline Flows Around a Circular Cylinder

S. Chono [a b] & T. Suji [a b]

[a] Department of Materials Science and Engineering, Fukui University, Fukui, 910, Japan

[b] Kochi University of Technology, Tosayamada, Kochi, 782, Japan

Version of record first published: 04 Oct 2006

To cite this article: S. Chono & T. Suji (1998): Numerical Simulation of Nematic Liquid Crystalline Flows Around a Circular Cylinder, Molecular Crystals and Liquid Crystals Science and Technology. Section A. Molecular Crystals and Liquid Crystals, 309:1, 217-236

To link to this article: http://dx.doi.org/10.1080/10587259808045530

Mol. Cryst. Liq. Cryst., 1998, Vol. 309, pp. 217–236
Reprints available directly from the publisher
Photocopying permitted by license only

Numerical Simulation of Nematic Liquid Crystalline Flows Around a Circular Cylinder

SHIGEOMI CHONO* and TOMOHIRO TSUJI*

Department of Materials Science and Engineering, Fukui University, Fukui 910, Japan

(Received 7 October 1996; In final form 23 July 1997)

Numerical solutions to the full set of partial differential equations for the Leslie-Ericksen theory are obtained for steady flows of non-tumbling nematic liquid crystals around a circular cylinder with an infinite axial length. The streamline pattern for fixed director orientation, which has been presented by Heuer *et al.*, differs from our results, which are obtained without approximations. An upstream displacement of the streamlines is observed for small Ericksen numbers. This streamline displacement is shifted to the downstream region with increasing the Ericksen number because the effect of fluid inertia becomes large. The distinctive director orientation profile is predicted in the downstream region of a circular cylinder when the Ericksen number is large. Flow kinematics such as streamline pattern and director orientation profile change greatly between the Ericksen number of 10 and 50 for a planar anchoring configuration. For a homeotropic anchoring configuration, on the other hand, the effect of Ericksen number is suppressed in the present calculation. The orientation angle of the director relative to the streamline along the specific streamline explains successfully the relationship between director orientation and streamline patterns.

Keywords: Nematic liquid crystal; finite difference method; flow around a circular cylinder; Leslie-Ericksen theory

1. INTRODUCTION

Nematic liquid crystals have a microstructure in which molecules are oriented in a certain direction but their positions are random. There are two available theories for the rheology of nematic liquid crystals; one is the

* Present address: Kochi University of Technology, Tosayamada, Kochi 782, Japan.

Leslie-Ericksen theory [1–3] developed in 1960's based on continuum theory, and the other is the Doi theory [4, 5] developed in 1981 based on molecular dynamics.

Many calculations have been performed using the L-E theory [6–10]; de Gennes [11] and Leslie [12] have reviewed the theory and the calculated results in detail. Owing to the complexity of the L-E equations, however, such calculations have been concerned with simple geometries in which the L-E equations can be reduced to ordinary differential equations. Several authors have solved flow problems in complex geometries where the elastic stresses and torques are neglected, in which case the L-E theory simplifies to the Transversely Isotropic Fluid (TIF) [1, 2]. The first study to consider the full set of partial differential equations for the TIF is that of Vanderheyden and Ryskin [13]. Baleo *et al.* [14] obtained finite element solutions for a variety of axisymmetric flows. Recently, Güler [15] and Chang *et al.* [16] presented finite difference and finite element solutions respectively, in two-dimensional complex flows using the TIF approximation. A number of authors have also obtained numerical solutions in complex geometries for a theory of fiber suspensions which is equivalent to an ensemble-averaged TIF; see Rosenberg *et al.* [17] for an example and references to earlier work. The first study of the full set of partial differential equations for the L-E theory with the isotropic elasticity approximation is that of Mori *et al.* [18] on two-dimensional developing inlet flow between parallel plates. Recently, Chono *et al.* [19, 20] applied the full L-E equations to both 4 to 1 contraction flow and flow in L-shaped channels with various contraction ratios of upstream to downstream channel width.

Flow past a circular cylinder with infinite length is a classical problem and of both hydradynamic and industrial interest. The first study of this flow for nematic liquid crystals was made by Heuer *et al.* [21]. Considering nematic flows under strong external fields such as electric or magnetic fields, they introduced a simplification wherein the orientation angle of the director is uniform in the whole flow region and the wall anchoring at solid surfaces is weak, which is not only equivalent to the TIF approximation mentioned above but also makes solution of the angular momentum equation unnecessary. In this study, we remove this simplification and present numerical solutions to the full L-E equations for flows around a circular cylinder.

2. BASIC EQUATIONS AND BOUNDARY CONDITIONS

2.1. Basic Equations

The conservation equations for an isothermal incompressible Leslie-Ericksen nematic liquid are as follows:

i) continuity equation

$$\nabla \cdot \mathbf{v} = 0 \tag{1}$$

ii) linear momentum equation

$$\rho \frac{D\mathbf{v}}{Dt} = -\nabla p + \nabla \cdot \boldsymbol{\tau} \tag{2}$$

iii) angular momentum equation

$$\mathbf{0} = \mathbf{n} \times \left\{ \frac{\partial F}{\partial \mathbf{n}} - \nabla \cdot \left(\frac{\partial F}{\partial \nabla \mathbf{n}} \right) + \lambda_1 \mathbf{N} + \lambda_2 \mathbf{A} \cdot \mathbf{n} \right\} \tag{3}$$

$\mathbf{v}$ is the velocity vector, ρ the fluid density, D/Dt the material time derivative, p the pressure, and $\boldsymbol{\tau}$ the extra-stress tensor expressed as

$$\begin{aligned} \boldsymbol{\tau} = {} & \alpha_1 \mathbf{nnnn} : \mathbf{A} + \alpha_2 \mathbf{nN} + \alpha_3 \mathbf{Nn} + \alpha_4 \mathbf{A} \\ & + \alpha_5 \mathbf{nn} \cdot \mathbf{A} + \alpha_6 \mathbf{A} \cdot \mathbf{nn} - \frac{\partial F}{\partial \nabla \mathbf{n}} \cdot (\nabla \mathbf{n})^T \end{aligned} \tag{4}$$

where $\mathbf{n}$ is a unit vector defined as the average molecular orientation and called the *director*. $\alpha_i (i = 1 \sim 6)$ are the Leslie viscosities and $\mathbf{A}$ is the rate of deformation tensor

$$\mathbf{A} = \frac{1}{2} \left\{ (\nabla \mathbf{v})^T + \nabla \mathbf{v} \right\} \tag{5}$$

$\mathbf{N}$ is the director angular velocity relative to that of the fluid and defined as

$$\mathbf{N} = \frac{\mathscr{D}\mathbf{n}}{\mathscr{D}t} \equiv \frac{D\mathbf{n}}{Dt} - \boldsymbol{\Omega} \cdot \mathbf{n} \tag{6}$$

where $\mathscr{D}/\mathscr{D}t$ is the Jaumann derivative and $\mathbf{\Omega}$ is the vorticity tensor

$$\mathbf{\Omega} = \frac{1}{2}\left\{(\nabla \mathbf{v})^T - \nabla \mathbf{v}\right\} \tag{7}$$

F in Equations (3) and (4) is the free energy density caused by the spatial distortion of the director;

$$2F = K_1(\nabla \cdot \mathbf{n})^2 + K_2(\mathbf{n} \cdot \nabla \times \mathbf{n})^2 + K_3|\mathbf{n} \times \nabla \times \mathbf{n}|^2 \tag{8}$$

where K_1, K_2 and K_3 are elastic constants corresponding to splay, twist and bend deformations of the director field, respectively. λ_1 and λ_2 are related to the Leslie viscosity as follows:

$$\lambda_1 = \alpha_3 - \alpha_2 \tag{9a}$$

$$\lambda_2 = \alpha_6 - \alpha_5 \tag{9b}$$

The equations for the TIF (Transversely Isotropic Fluid) are obtained by eliminating the free energy terms from Equations (3) and (4).

Züñiga and Leslie [22, 23] did a stability analysis of the Sturm-Liouville eigenvalue problem and showed that the director moves out of the shear plane as the shear rate is increased. They [24] also extended the analysis to plane Poiseuille flow. Han and Rey [25, 26] analyzed an unsteady phenomenon of out-of-plane for the director. However, as far as two-dimensional calculations for the TIF [13–16] are concerned, the in-plane assumption has been used for the director. In the present analysis, we also assume that the director $\mathbf{n}$ lies in the sample plane as that of the velocity field. Thus, in a planar cylindrical coordinate system ($r-\theta$), as shown in Figure 1, where the flow around a circular cylinder is best described, $\mathbf{n}$ is expressed as

$$\mathbf{n} = (\cos\phi, \sin\phi)^T \tag{10}$$

ϕ is the orientation angle of the director with respect to a r-axis at angle θ from the x-axis. After Equations (2)–(8) without unsteady terms were reduced to the form of the r-θ coordinates of Figure 1 using a mathematical software "REDUCE", we introduced a streamfunction ψ, and non-dimensionalized with the cylinder radius a, the uniform velocity U at the infinity, the viscosity α_4 and the elastic constant K_1. Hereafter, all physical

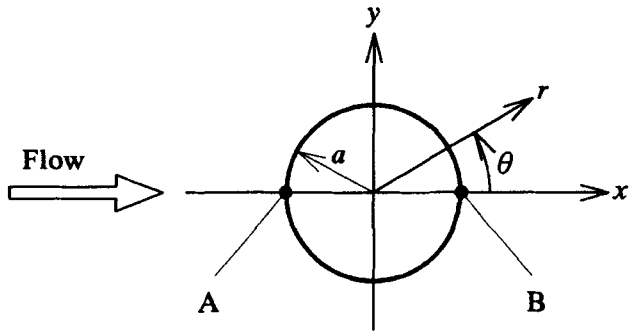

FIGURE 1 Flow geometry and coordinate system.

quantities are to be considered in their dimensionless forms. Then we concentrated grid points near the cylinder, where greater accuracy was necessary, and also lengthened the regions far from the cylinder without increasing the number of grid points by introducing the transformation

$$r = e^{\xi} \tag{11}$$

to obtain the resulting equations;

$$\mathrm{Re}\, e^{\xi}\left(u\frac{\partial\omega}{\partial\xi}+v\frac{\partial\omega}{\partial\theta}\right)=\nabla^2\omega+\frac{f(\phi)}{\mathrm{Er}}+g(\psi,\phi) \tag{12}$$

$$\begin{aligned}\mathrm{Er}\, e^{\xi}\lambda_1\left(u\frac{\partial\phi}{\partial\xi}+v\frac{\partial\phi}{\partial\theta}\right)&=\frac{1+K_3}{2}\nabla^2\phi\\&+\frac{1-K_3}{2}\sin 2\phi\left\{\left(\frac{\partial\phi}{\partial\xi}\right)^2-2\frac{\partial^2\phi}{\partial\xi\partial\theta}-\left(\frac{\partial\phi}{\partial\theta}\right)^2+1\right\}\\&-\frac{1-K_3}{2}\cos 2\phi\left(\frac{\partial^2\phi}{\partial\xi^2}+2\frac{\partial\phi}{\partial\xi}\frac{\partial\phi}{\partial\theta}-\frac{\partial^2\phi}{\partial\theta^2}\right)\\&+\mathrm{Er}\,\lambda_1\left(\frac{1}{2}e^{2\xi}\omega+\frac{\partial\psi}{\partial\xi}\right)\\&+\mathrm{Er}\,\lambda_2\left\{\left(\frac{\partial^2\psi}{\partial\xi\partial\theta}-\frac{\partial\psi}{\partial\theta}\right)\sin 2\phi+\frac{1}{2}e^{2\xi}\omega\cos 2\phi\right\}\end{aligned} \tag{13}$$

$$\frac{\partial^2\psi}{\partial\xi^2}+\frac{\partial^2\psi}{\partial\theta^2}=-e^{2\xi}\omega \tag{14}$$

where u and v are the ξ and θ components of the velocity, respectively, and ω is the vorticity. Re is the Reynolds number, and Er is the Ericksen number which represents the ratio of viscous to elastic forces; the dimensionless groups are defined as follows;

$$\mathrm{Re} = \frac{\rho a U}{\alpha_4} \tag{15a}$$

$$\mathrm{Er} = \frac{\alpha_4 a U}{K_1} \tag{15b}$$

The expressions for $f(\phi)$ and $g(\psi, \phi)$ in Equation (12) are given in the Appendix. We may choose an alternative but equivalent expression for the extra-stress tensor Equation (4). In such a case, the term $f(\phi)$ can be eliminated but the term $g(\psi, \phi)$ becomes more complicated; see Leslie [27].

2.2. Boundary Conditions

To complete the specification of the problem, we require appropriate boundary conditions for velocity and director orientation fields. Since we will consider cylindrical profiles which are symmetric with respect to the x-axis as shown in Figure 1, only the half space of the flow domain is needed to be solved by setting the boundary conditions on the centerline as well as along the cylinder surface and at infinity.

For the velocity field, we have a no-slip condition along the cylinder surface and a uniform flow profile in the positive x direction at infinity; that is,

$$u = v = 0 \quad \text{at} \quad r = a \tag{16}$$

$$u = U\cos\theta, \quad v = -U\sin\theta \quad \text{at} \quad r = R \tag{17}$$

where $R \gg a$. On the centerline,

$$\frac{\partial u}{\partial \theta} = v = 0 \tag{18}$$

from symmetry.

For the orientation field of the director, the alignment direction is indeterminate in the uniform velocity profile at the upstream region. Here,

in order to facilitate the imposition of an orientation boundary condition and also to make it physically meaningful at the upstream region, we implicitly assume the existence of a considerably weak magnetic field parallel to the x direction at large distances upstream. Though the external field is so weak that it has little effect on the flow behavior near the cylinder, it can easily orient the director to the x direction at the upstream region, because there is no aligning agency (for example, velocity gradients, solid boundaries, etc.) except it. Therefore, we set the director parallel to the x direction at upstream infinity ($\pi/2 \leq \theta \leq \pi$), while no changes in the main flow direction are imposed on the outlet ($0 \leq \theta \leq \pi/2$); that is,

$$\phi = -\theta \quad \text{at} \quad r = R, \quad \frac{\pi}{2} \leq \theta \leq \pi \tag{19}$$

$$\frac{\partial \phi}{\partial x} = 0 \quad \text{at} \quad r = R, \quad 0 \leq \theta \leq \frac{\pi}{2} \tag{20}$$

The anchoring angle along the cylinder surface ϕ_w was considered as one of the calculation parameters; we selected two kinds of typical situations, one being the director which is tangential to the cylinder surface, that is, $\phi_w = -\pi/2$ (planar configuration), and the other being the case where the director is normal to the surface, that is, $\phi_w = -\pi$ (homeotropic configuration). Along the centerline, Baleo *et al.* [14] have reported that the director shows a transverse orientation before an obstacle and is aligned with the centerline after the obstacle because of acceleration. However, this is the conclusion for the TIF, which has no spatial orientation restriction caused by the elasticity of the director field, and for flow through a tube, where the effect of deceleration and acceleration is large; thus, it seems to be difficult to apply directly such a condition to the present study. As a result of solving the whole flow region without using the centerline boundary conditions at $\mathrm{Er} = 10$ for planar configuration, for example, we obtained the aligned orientation on the centerline. So, we use the following condition:

$$\left.\begin{aligned} \phi &= 0 \quad \text{at} \quad \theta = 0 \\ \phi &= -\pi \quad \text{at} \quad \theta = \pi \end{aligned}\right\} \quad \text{for} \quad \phi_w = -\frac{\pi}{2} \tag{21}$$

$$\left.\begin{aligned} \phi &= -\pi \quad \text{at} \quad \theta = 0 \\ \phi &= -\pi \quad \text{at} \quad \theta = \pi \end{aligned}\right\} \quad \text{for} \quad \phi_w = -\pi \tag{22}$$

It should be noted that taking into account that the flow kinematics are symmetric with respect to the x-axis, determination of the anchoring angles

at stagnation points (points A and B in Fig. 1) is a serious problem for the planar configuration. It is found from some preliminary calculations that when the Ericksen number is less than unity, the effect of the anchoring angles at only the two points is large, but for the Ericksen number more than 5, flow kinematics are independent of the angles at those points. Therefore, for simplicity, we considered such points to be on the centerline.

3. NUMERICAL METHOD

Calculations were performed by the finite difference method. When the Ericksen number Er is 100, which is the maximum value with the present calculation, ξ in Equation (11) is taken to be 5.3 giving an outer radius R of 200, and for the other cases of smaller Ericksen numbers, we take $\xi = 5$ giving $R = 148$. Before making the main calculations, we investigated the effect of mesh refinement for $\mathrm{Er} = 10$ using three different mesh sizes, 90×60, 120×90 and 180×180 in the ξ and θ directions, respectively. Though a slight difference in streamlines is discernible between the coarse mesh and the intermediate one, we cannot find any difference between the intermediate mesh and the fine one. Further mesh refinement is assumed not to lead to appreciable differences in flow kinematics, and we employed 120×90 grid points in later calculations. For $\mathrm{Er} = 100$, however, 180×180 grid points were used because of a wider calculation area.

The nonlinear coupled system for ω, ψ, and ϕ resulting from the discretization of the governing equations is linearized by a separate treatment of each equation. The SOR iteration is used to solve the linear system. It is assumed that convergence is obtained when the following inequalities for relative changes averaged over the nodal points are satisfied:

$$\frac{1}{N}\sum_{i,j}^{N}\left|\frac{\omega_{i,j}^{n+1}-\omega_{i,j}^{n}}{\omega_{i,j}^{n}}\right| < 10^{-5} \tag{23}$$

$$\frac{1}{N}\sum_{i,j}^{N}\left|\frac{\psi_{i,j}^{n+1}-\psi_{i,j}^{n}}{\psi_{i,j}^{n}}\right| < 10^{-6} \tag{24}$$

$$\frac{1}{N}\sum_{i,j}^{N}\left|\frac{\phi_{i,j}^{n+1}-\phi_{i,j}^{n}}{\phi_{i,j}^{n}}\right| < 10^{-6} \tag{25}$$

where N is the total nodal number and superscripts n and $n+1$ mean iteration number. We have no flow instabilities in the present calculations, because the Ericksen number is not high, and the velocity gradient is moderate in flow around an obstacle (a circular cylinder) in comparison with flow in channels.

The physical constants for *p*-azoxyanisole (PAA) are tabulated in Table I. The data in this table are those used by Tseng *et al.* [7] and are dimensional. The value of K_2 is not necessary when the director lies in its orientation plane. It is clear from Equations (9) and (10) that the Reynolds and Ericksen numbers can be varied only by the flow rate for fixed physical constants. Therefore, each is dependent on the other, and Re is less than Er by a factor of 10^4 in the present calculations. The fluid density ρ is 1000 kg/m^3.

4. RESULTS AND DISCUSSION

4.1. Streamline for Fixed Director Orientation

As mentioned in the Introduction, Heuer *et al.* [21] made an assumption that strong external forces induced by electric or magnetic fields are exerted on the system and it has weak anchoring at the solid surface, so that the director can orient at an arbitrary angle along the wall, resulting in the situation that the director profile is homogeneous in the whole flow domain, including the cylinder surface. Under such a condition, the angular momentum equations is not required and also the linear momentum equation reduces to a considerably simpler form, because the orientation angle of the director is no longer an unknown variable. Before showing the solution to the full set of the L-E equations, we present some results obtained under the fixed director orientation assumption.

Streamlines with the director parallel and perpendicular to the x-axis are indicated in the upper- and lower-half of Figure 2 for a Reynolds number of $\mathrm{Re} = 10^{-3}$. Values of streamfunctions are 0 on the centerline and increase by a step of 0.1 with increasing the distance from the cylinder. Because the

TABLE I Physical constants

Viscosities $\times 10^3$ *Pa s*						*Elastic constants* $\times 10^{12}$ *N*	
α_1	α_2	α_3	α_4	α_5	α_6	K_1	K_3
4.3	− 6.9	− 0.2	6.8	4.7	− 2.3	4.9	10.5

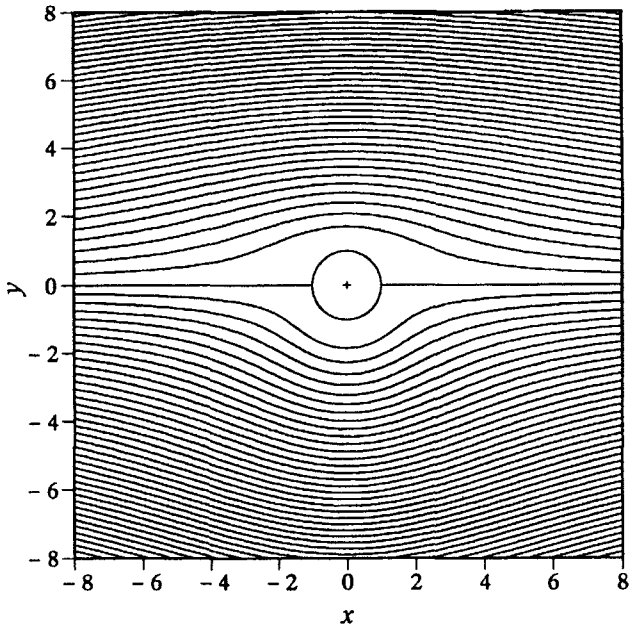

FIGURE 2 Streamlines for fixed director orientation at $Re = 10^{-3}$. The upper-half is for the director parallel to the x-axis and the lower-half is for the director perpendicular to the x-axis. Values of streamfunctions are 0 on the centerline and increase by a step of 0.1 with increasing the distance from the cylinder.

director orientation is uniform in the whole flow region, and also Re is very low, which corresponds nearly to Stokes flow, streamlines are observed to be symmetric with respect to the y-axis. For the director orientation parallel to the x-axis, streamlines are distorted at a further upstream region, so that the fluid passes around the cylinder smoothly. In contrast, when the director is fixed perpendicular to the x-axis, the profile of streamlines reflects the shape of a circle, and the fluid turns abruptly close to the cylinder. This is because when the fluid is forced to have a y-component of velocity due to the presence of a circular cylinder, the director orientation parallel to the x-axis suppresses such a behavior, and the director orientation perpendicular to the x-axis acts to facilitate the behavior. In addition to the difference in streamlines, the pressure gradient in the main flow direction is different for the two cases.

It is clear that the streamlines for a Newtonian fluid at the same Reynolds number show an intermediate pattern between the two cases. Therefore, it is confirmed that the director orientation has a large effect on the velocity field, and that the director and velocity fields must be solved simultaneously.

4.2. Flow Around a Circular Cylinder

Figure 3 shows the streamlines and the director profiles for Er = 5, 10, 50 and 100, when the anchoring angle $\phi_w = -\pi/2$ (planar configuration). Values of streamfunctions are identical to those of Figure 2. For Er = 5, the director with the orientation angle almost parallel to the x direction in the upstream region passes around the cylinder smoothly, and the spatial variation in the director orientation is not so remarkable over the entire flow region except for a small area near the cylinder. In spite of a low Reynolds number of $\mathrm{Re} = 5\times10^{-4}$, streamlines are not symmetric with respect to the y-axis, and a

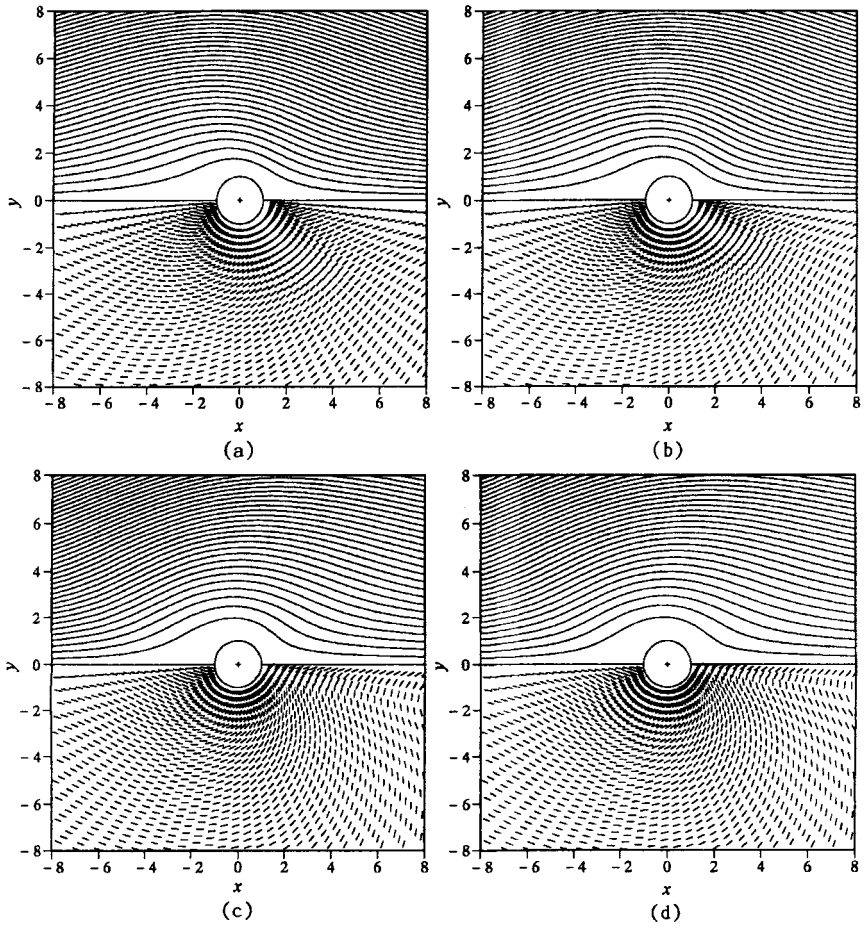

FIGURE 3 Streamlines and director profiles for the anchoring angle $\phi_w = -\pi/2$. (a) Er = 5; (b) Er = 10; (c) Er = 50; (d) Er = 100. Values of streamfunctions are identical to those of Figure 2.

streamline displacement to the upstream region can be observed, which is considerably different from the results in Figure 2. This is obviously due to the distribution of director orientation. As Er is increased to 10, no great differences are noted in velocity and director orientation fields, though the streamline displacement to the upstream region is suppressed compared with that for Er = 5. However, when Er is increased further to 50, significant changes are observed both in the streamline pattern and in the director orientation profile; the upstream displacement of streamline is confined in a narrow region near the cylinder, and a downstream displacement occurs at an area far from the cylinder. The curvature of streamlines near the cylinder becomes large, which is similar to the streamline with the director perpendicular to the x-axis in Figure 2. The director orientation profile in the upstream area of the cylinder is essentially identical to that for the lower Er, but in the downstream region of the cylinder, especially behind it, the director shows its involution into the rear of the cylinder. The streamline displacement to the downstream and the orientation profile of the director and enhanced at Er = 100; in particular, the director rotates behind the cylinder and is moved to the downstream where it behaves like a kite released from a string, because the velocity gradient is very small in this place.

It is of some interest that for every Er, the director already has a positive y-component in an upstream area (if we draw the director orientation profile in the upper-half space of Figures in order to superpose it upon streamlines, the director is found to make a negative angle with respect to streamlines; here, we define a counterclockwise rotation of the director with respect to streamlines as a positive one). The orientation angle of the director relative to the streamline along the specific streamline gives a comprehensive explanation for the relationship between director orientation streamlines. The relative orientation angles ϕ_r along streamlines for streamfunctions of 0.01, 0.1 and 1 are plotted as a function of x in Figure 4. It is found that a different tendency is obtained between Er = 10 and 50, which is the same as the results of Figure 3. In the case that only shear flow exists and that the anchoring effect is negligible, the director makes an angle ϕ_L with respect to streamlines, given as

$$\tan^2\phi_L = \frac{\alpha_3}{\alpha_2} \tag{26}$$

which is called the Leslie angle (= 9.7 deg for PAA). Owing to the presence of a cylinder, streamlines are curved to the positive y direction upstream of the cylinder. However, since the director orientation along the curved

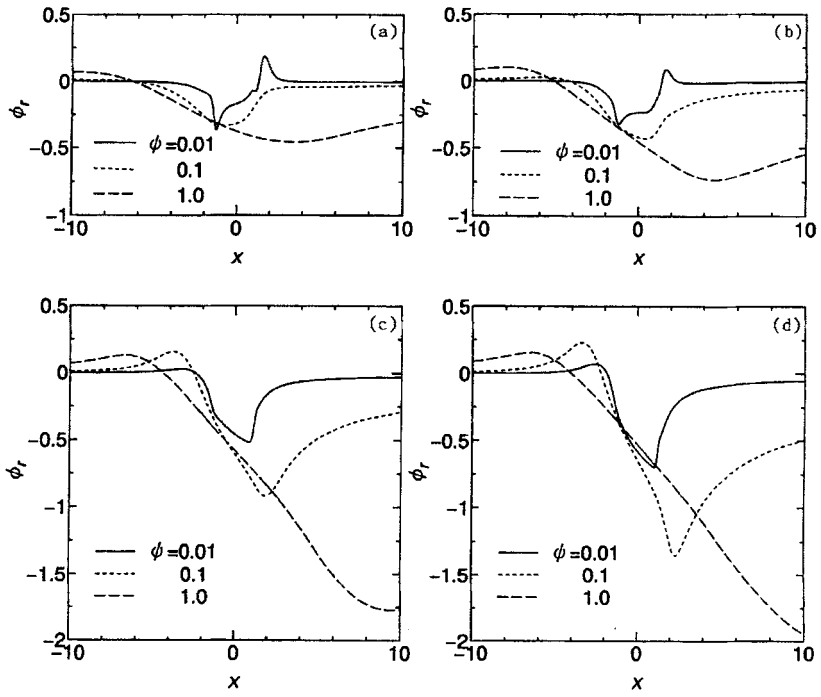

FIGURE 4 Relative orientation angles ϕ_r with respect to streamlines for the anchoring angle $\phi_w = -\pi/2$. (a) Er = 5; (b) Er = 10; (c) Er = 50; (d) Er = 100. Streamfunctions selected are 0.01, 0.1 and 1.0.

streamlines increases the free energy density due to the bend deformation of director field, the director cannot orient along the streamlines, but takes a negative relative angle upstream of the cylinder as shown in Figure 4. Once this angle becomes below $-\phi_L$, the viscosity torque due to velocity gradient acting on the director changes its sign to positive, and the director rotates clockwise. This is the reason why ϕ_r is negative in an area upstream the cylinder. Downstream, for Er = 5, where the Frank elasticity which suppresses the spatial distortion of the director is dominant, it is observed that ϕ_r does not have a value so far from 0 deg and even shows a positive value on the streamline $\psi = 0.01$. At Er = 50 and 100, on the other hand, ϕ_r approaches 0 deg along the streamlines $\psi = 0.01$ and 0.1, and shows a monotonic decrease along $\psi = 1$.

Upstream and downstream displacements of streamlines were already observed in Figure 3. Here, we investigate the displacements in detail as a function of Ericksen number. Figure 5 shows the streamline displacement L,

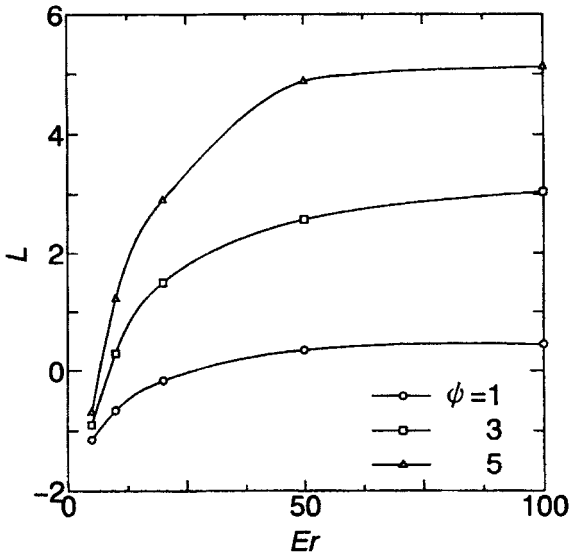

FIGURE 5 Streamline displacements L as a function of Er for the anchoring angle $\phi_w = -\pi/2$. L is defined as the x-coordinate where the maximum in the y-coordinate for a streamline occurs, the positive value meaning a shift to the downstream, and the negative value corresponding to a shift to the upstream.

which is defined as the x-coordinate where the maximum in the y-coordinate for a streamline occurs, the positve value meaning a shift to the downstream, and the negative value corresponding to a shift to the upstream. For small Er, L shows a negative value. Similar behavior has been obtained theoretically and experimentally by Ultman and Denn [28], and experimentally by Manero and Mena [29] for viscoelastic flow. In the present case, director orientation is assumed to be largely responsible for such results; as indicated in Figure 3, the director has already a positive y-component upstream of the cylinder. Thus, it is understood that the peak of a curved streamline occurs upstream of the cylinder. As Er increases, L increases to a positive value and is finally saturated at large Er.

In order to investigate the effect of anchoring angle on flow behavior, we give the streamlines and the director orientation profiles in Figure 6 and the relative director orientation angle ϕ_r in Figure 7 with the anchoring angle of $\phi_w = -\pi$ (homeotropic configuration) for Er = 10 and 50. In Figure 6, values of streamfunctions are identical to those of Figure 2. Since this type of director anchoring is resistant to flow around a cylinder, the curvature of streamlines around it becomes large and the streamline pattern is similar to that with the director perpendicular to the x-axis in Figure 2. The director

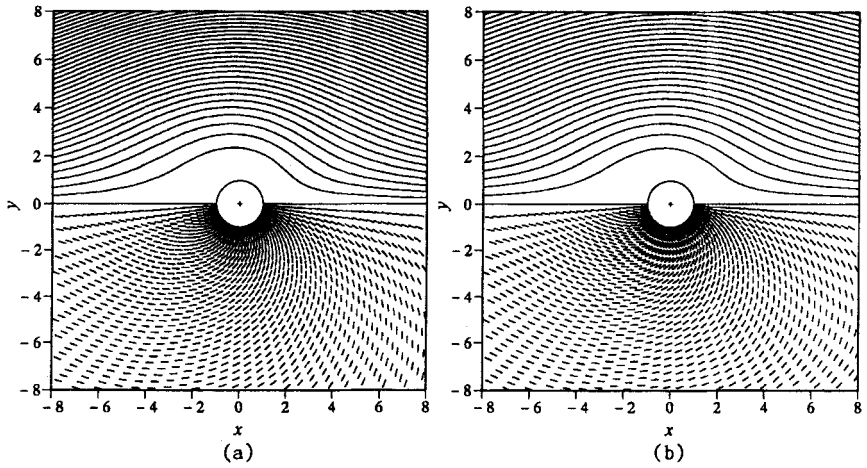

FIGURE 6 Streamlines and director profiles for the anchoring angle $\phi_w = -\pi$. (a) Er = 10; (b) Er = 50. Values of streamfunctions are identical to those of Figure 2.

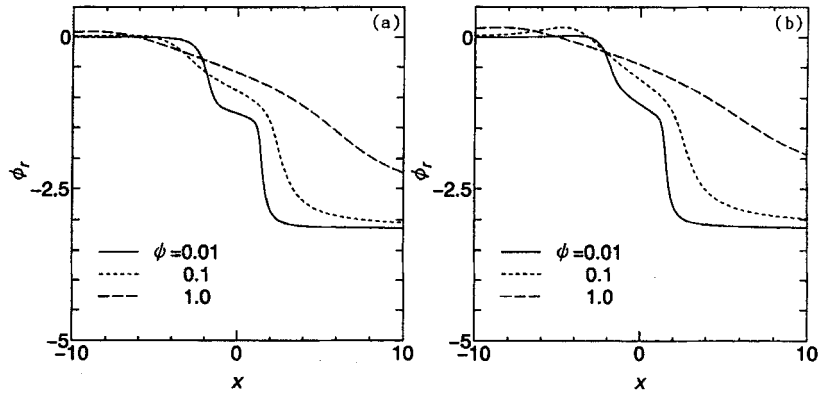

FIGURE 7 Relative orientation angles ϕ_r with respect to streamlines for the anchoring angle $\phi_w = -\pi$. (a) Er = 10; (b) Er = 50. Streamfunctions selected are 0.01, 0.1 and 1.0.

orientation downstream of the cylinder is completely opposite to that in the upstream region, so that the spatial variation in the director orientation profile seems to be quite large in the whole flow region. Thus, the effect of the Ericksen number is not so remarkable compared with the results in Figure 3 for planar configuration. In reflecting the small effect of Er, the variation in relative orientation angle ϕ_r is also approximately identical to each other between Er = 10 and 50. Comparison with Figure 4 leads to the fact that at Er = 10, the director along three streamlines shown in Figure 7 is

influenced by anchoring angle, while at Er = 50, where the effect of the Frank elasticity is confined near wall surface, the director orientation along the streamline $\psi = 1$ is independent of director anchoring angle.

5. CONCLUSIONS

This paper reports the nematic liquid crystalline flow around a circular cylinder with an infinite axial length using the Leslie-Ericksen equations. At low Ericksen numbers, an upstream displacement of the streamlines is predicted. This streamline displacement is shifted to the downstream region with increasing Ericksen number because the effect of fluid inertia becomes large. These results for streamline are considerably different from those obtained by Heuer *et al.* with an assumption that the directior is fixed in a certain direction. A distinctive director orientation profile is predicted in the downstream region of a circular cylinder when the Ericksen number is large. Streamline pattern and director orientation are changed remarkably at Ericksen numbers between 10 and 50 for a planar anchoring configuration. For a homeotropic anchoring configuration, on the other hand, the effect of Ericksen number is small, because the spatial variation in the director orientation profile is largely independent of Ericksen number. The orientation angle of the director relative to the streamline along the specific streamline explains successfully the relationship between director orientation and streamline patters.

References

[1] J. L. Ericksen, *Arch. Ration. Mech. Anal.*, **4**, 231 (1960).
[2] J. L. Ericksen, *Trans. Soc. Rheol.*, **5**, 23 (1961).
[3] F. M. Leslie, *Arch. Ration. Mech. Anal.*, **28**, 265 (1968).
[4] M. Doi, *J. Poly. Sci. Phys. Ed.*, **19**, 229 (1981).
[5] M. Doi and S. F. Edwards, *The theory of polymer dynamics*, Clarendon Press, Oxford, (1986).
[6] P. K. Currie, *Arch. Ration. Mech. Anal.*, **37**, 222 (1970).
[7] H. C. Tseng, D. L. Silver and A. B. Finlayson, *Phys. Fluids*, **15**, 1213 (1972).
[8] P. K. Currie, *Rheol. Acta.*, **14**, 688 (1975).
[9] A. D. Rey and M. M. Denn, *J. Non-Newtonian Fluid Mech.*, **27**, 37 (1988).
[10] A. D. Rey, *J. Rheol.*, **34**, 425 (1990).
[11] P. G. de Gennes, *The physics of liquid crystals*, Oxford Univ. Press (1974).
[12] F. M. Leslie, *Adv. Liq. Cryst.*, **4**, 1 (1979).
[13] W. B. Vanderheyden and G. Ryskin, *J. Non-Newtonian Fluid Mech.*, **23**, 383 (1987).
[14] J. N. Baleo, M. Vincent, P. Navard and Y. Demay, *J. Rheol.*, **36**, 663 (1992).
[15] M. Güler, *J. Non-Newtonian Fluid Mech.*, **52**, 309 (1994).
[16] R. Y. Chang, F. C. Shiao and W. L. Yang, *J. Non-Newtonian Fluid Mech.*, **55**, 1 (1994).
[17] J. Rosenberg, M. M. Denn and R. Keunings, *J. Non-Newtonian Fluid Mech.*, **37**, 317 (1990).

[18] N. Mori, M. Fukui and K. Nakamura, *Trans. Japan Soc. Mech. Eng.*, **59**, 1049 (in Japanese) (1993).
[19] S. Chono, T. Tsuji and M. M. Denn, *Trans. Japan Soc. Mech. Eng.*, **60**, 1944 (in Japanese) (1994).
[20] S. Chono and T. Tsuji, *Trans. Japan Soc. Mech. Eng.*, **61**, 1600 (in Japanese) (1995).
[21] H. Heuer, H. Kneppe and F. Schneider, *Mol. Cryst. Liq. Cryst.*, **200**, 51 (1991).
[22] I. Züñiga and F. M. Leslie, *Europhys. Lett.*, **9**, 689 (1989).
[23] I. Züñiga and F. M. Leslie, *Liq. Cryst.*, **5**, 725 (1989).
[24] I. Züñiga and F. M. Leslie, *J. Non-Newtonian Fluid Mech.*, **33**, 123 (1989).
[25] W. H. Han and A. D. Rey, *J. Non-Newtonian Fluid Mech.*, **48**, 181 (1993).
[26] W. H. Han and A. D. Rey, *J. Non-Newtonian Fluid Mech.*, **50**, 1 (1993).
[27] F. M. Leslie, IMA 5, Theory and applications of liquid crystals, Springer Verlag, 235 (1989).
[28] J. S. Ultman and M. M. Denn, *Chem. Eng. J.*, **2**, 81 (1971).
[29] O. Manero and B. Mena, *J. Non-Newtonian Fluid Mech.*, **9**, 379 (1981).

APPENDIX

The expressions for $f(\phi)$ and $g(\psi, \phi)$ in Equation (12) are presented. The subscript denotes partial derivative with respect to it. The authors are ready to supply Equations (12) and (13) in the form of Cartesian (2-D and 3-D), planar cylindrical and polar coordinate systems on a diskette if required.

$$
\begin{aligned}
f = & -\cos2\phi\phi_\xi + \cos2\phi\phi_{\theta\theta}\phi_\theta + \cos2\phi\phi_{\theta\theta} - 1/2\phi_{\xi\theta\theta}\phi_\theta - 1/2\phi_{\xi\theta\theta} \\
& - 1/2\phi_{\xi\xi\xi}\phi_\theta - 1/2\phi_{\xi\xi\xi} + 1/2\phi_{\xi\xi\theta}\phi_\xi + \phi_{\xi\xi}\phi_\theta + \phi_{\xi\xi} + 1/2\phi_\xi\phi_{\theta\theta\theta} + \phi_{\theta\theta}\phi_\theta \\
& + \phi_{\theta\theta} - \sin2\phi\phi_{\xi\theta\theta}\phi_\xi + \sin2\phi\phi_{\xi\theta}\phi_\xi^2 + \sin2\phi\phi_{\xi\theta}\phi_\phi^2 - \sin2\phi\phi_{\xi\theta}\phi_\theta - 2\sin2\phi\phi_{\xi\theta} \\
& + \sin2\phi\phi_{\xi\xi\theta}\phi_\theta + \sin2\phi\phi_{\xi\xi\theta} - \sin2\phi\phi_{\xi\xi}\phi_\xi\phi_\theta - 2\sin2\phi\phi_{\xi\xi}\phi_\xi - \sin2\phi\phi_\xi^2\phi_\theta \\
& + \sin2\phi\phi_\xi^2 - \sin2\phi\phi_\xi\phi_{\theta\theta}\phi_\theta + \sin2\phi\phi_\xi\phi_{\theta\theta} - \sin2\phi\phi_\theta^2 - \sin2\phi\phi_\theta^2 + \sin2\phi\phi_\theta \\
& + \sin2\phi - 1/2\cos2\phi\phi_{\xi\theta\theta}\phi_\theta - 1/2\cos2\phi\phi_{\xi\theta\theta} + 3\cos2\phi\phi_{\xi\theta}\phi_\xi \\
& + 1/2\cos2\phi\phi_{\xi\xi\xi}\phi_\theta + 1/2\cos2\phi\phi_{\xi\xi\xi} - 1/2\cos2\phi\phi_{\xi\xi\theta}\phi_\xi + \cos2\phi\phi_{\xi\xi}\phi_\theta^2 \\
& - \cos2\phi\phi_{\xi\xi} - \cos2\phi\phi_\xi^3 - \cos2\phi\phi_\xi^2\phi_{\theta\theta} + 1/2\cos2\phi\phi_\xi\phi_{\theta\theta\theta} - \cos2\phi\phi_\xi\phi_\theta^2 \\
& - 2\cos2\phi\phi_\xi\phi_\theta + K_3(-\cos2\phi\phi_{\theta\theta}\phi_\theta - \cos2\phi\phi_{\theta\theta} - 1/2\phi_{\xi\theta\theta}\phi_\theta - 1/2\phi_{\xi\theta\theta} \\
& - 1/2\phi_{\xi\xi\xi}\phi_\theta - 1/2\phi_{\xi\xi\xi} + 1/2\phi_{\xi\xi\theta}\phi_\xi + \phi_{\xi\xi}\phi_\theta + \phi_{\xi\xi} + 1/2\phi_\xi\phi_{\theta\theta\theta} + \phi_{\theta\theta}\phi_\theta \\
& + \phi_{\theta\theta} + \sin2\phi\phi_{\xi\theta\theta}\phi_\xi - \sin2\phi\phi_{\xi\theta}\phi_\xi^2 - \sin2\phi\phi_{\xi\theta}\phi_\theta^2 + \sin2\phi\phi_{\xi\theta}\phi_\theta \\
& + 2\sin2\phi\phi_{\xi\theta} - \sin2\phi\phi_{\xi\xi\theta}\phi_\theta - \sin2\phi\phi_{\xi\xi\theta} + \sin2\phi\phi_{\xi\xi}\phi_\xi\phi_\theta + 2\sin2\phi\phi_{\xi\xi}\phi_\xi \\
& + \sin2\phi\phi_\xi^2\phi_\theta - \sin2\phi\phi_\xi^2 + \sin2\phi\phi_\xi\phi_{\theta\theta}\phi_\theta - \sin2\phi\phi_\xi\phi_{\theta\theta} + \sin2\phi\phi_\theta^2 \\
& + \sin2\phi\phi_\theta^2 + \sin2\phi\phi_\theta - \sin2\phi + 1/2\cos2\phi\phi_{\xi\theta\theta}\phi_\theta + 1/2\cos2\phi\phi_{\xi\theta\theta} \\
& - 3\cos2\phi\phi_{\xi\theta}\phi_\xi - 1/2\cos2\phi\phi_{\xi\xi\xi}\phi_\theta - 1/2\cos2\phi\phi_{\xi\xi\xi} + 1/2\cos2\phi\phi_{\xi\xi\theta}\phi_\xi
\end{aligned}
$$

$$
\begin{aligned}
&- \cos2\phi\phi_{\xi\xi}\phi_\theta^2 + \cos2\phi\phi_{\xi\xi} + \cos2\phi\phi_\xi^3 + \cos2\phi\phi_\xi^2\phi_{\theta\theta} - 1/2\cos2\phi\phi_\xi\phi_{\theta\theta\theta} \\
&+ \cos2\phi\phi_\xi\phi_\theta^2 + 2\cos2\phi\phi_\xi\phi_\theta + \cos2\phi\phi_\xi) \\
g =&\alpha_1(-2\cos2\phi\cos2\phi\psi_{\xi\xi}\phi_\xi^2 + 2\cos2\phi\cos2\phi\psi_{\xi\xi}\phi_\theta^2 - 3\cos2\phi\cos2\phi\psi_{\xi\xi}\phi_\theta \\
&- 2\cos2\phi\cos2\phi\psi_\xi\phi_{\xi\theta} + 4\cos2\phi\cos2\phi\psi_\xi\phi_\xi^2 - 4\cos2\phi\cos2\phi\psi_\xi\phi_\theta^2 \\
&+ 2\cos2\phi\cos2\phi\psi_\xi\phi_\theta - \cos2\phi\cos2\phi\psi_{\theta\theta\theta}\phi_\xi - \cos2\phi\cos2\phi\psi_{\theta\theta}\phi_{\xi\theta} \\
&+ 2\cos2\phi\cos2\phi\psi_{\theta\theta}\phi_\xi^2 - 2\cos2\phi\cos2\phi\psi_{\theta\theta}\phi_\theta^2 + 3\cos2\phi\cos2\phi\psi_{\theta\theta}\phi_\theta \\
&- \cos2\phi\cos2\phi\psi_{\theta\theta} - \cos2\phi\cos2\phi\psi_\theta\phi_{\xi\xi} - 8\cos2\phi\cos2\phi\psi_\theta\phi_\xi\phi_\theta \\
&+ 2\cos2\phi\cos2\phi\psi_\theta\phi_\xi + \cos2\phi\cos2\phi\psi_\theta\phi_{\theta\theta} + 16\sin2\phi\cos2\phi\psi_\xi\phi_\xi\phi_\theta \\
&- 4\sin2\phi\cos2\phi\psi_\xi\phi_\xi - 2\sin2\phi\cos2\phi\psi_\xi\phi_{\theta\theta} - 2\sin2\phi\cos2\phi\psi_{\theta\theta\theta}\phi_\theta \\
&+ \sin2\phi\cos2\phi\psi_{\theta\theta\theta} + \sin2\phi\cos2\phi\psi_{\theta\theta}\phi_{\xi\xi} + 8\sin2\phi\cos2\phi\psi_{\theta\theta}\phi_\xi\phi_\theta \\
&- 6\sin2\phi\cos2\phi\psi_{\theta\theta}\phi_\xi - \sin2\phi\cos2\phi\psi_{\theta\theta}\phi_{\theta\theta} - 4\sin2\phi\cos2\phi\psi_\theta\phi_{\xi\theta} \\
&+ 8\sin2\phi\cos2\phi\psi_\theta\phi_\xi^2 - 8\sin2\phi\cos2\phi\psi_\theta\phi_\theta^2 + 4\sin2\phi\cos2\phi\psi_\theta\phi_\theta \\
&- 3\cos2\phi\cos2\phi\psi_{\xi\theta\theta}\phi_\theta + 2\cos2\phi\cos2\phi\psi_{\xi\theta\theta} + \cos2\phi\cos2\phi\psi_{\xi\theta}\phi_{\xi\xi} \\
&+ 8\cos2\phi\cos2\phi\psi_{\xi\theta}\phi_\xi\phi_\theta - 6\cos2\phi\cos2\phi\psi_{\xi\theta}\phi_\xi - \cos2\phi\cos2\phi\psi_{\xi\theta}\phi_{\theta\theta} \\
&+ \cos2\phi\cos2\phi\psi_{\xi\xi\xi}\phi_\theta - \cos2\phi\cos2\phi\psi_{\xi\xi\theta\theta} + 3\cos2\phi\cos2\phi\psi_{\xi\xi\theta}\phi_\xi \\
&+ \cos2\phi\cos2\phi\psi_{\xi\xi}\phi_{\xi\theta} + 2\sin2\phi\sin2\phi\psi_{\theta\theta}\phi_\theta^2 - 3\sin2\phi\sin2\phi\psi_{\theta\theta}\phi_\theta \\
&+ \sin2\phi\sin2\phi\psi_\theta\phi_{\xi\xi} + 8\sin2\phi\sin2\phi\psi_\theta\phi_\xi\phi_\theta - 2\sin2\phi\sin2\phi\psi_\theta\phi_\xi \\
&- \sin2\phi\sin2\phi\psi_\theta\phi_{\theta\theta} - \sin2\phi\cos2\phi\psi_{\xi\theta\theta\theta} + 6\sin2\phi\cos2\phi\psi_{\xi\theta\theta}\phi_\xi \\
&+ 4\sin2\phi\cos2\phi\psi_{\xi\theta}\phi_{\xi\theta} - 8\sin2\phi\cos2\phi\psi_{\xi\theta}\phi_\xi^2 + 8\sin2\phi\cos2\phi\psi_{\xi\theta}\phi_\theta^2 \\
&- 12\sin2\phi\cos2\phi\psi_{\xi\theta}\phi_\theta + 2\sin2\phi\cos2\phi\psi_{\xi\theta} + \sin2\phi\cos2\phi\psi_{\xi\xi\xi\theta} \\
&- 2\sin2\phi\cos2\phi\psi_{\xi\xi\xi}\phi_\xi + 6\sin2\phi\cos2\phi\psi_{\xi\xi\theta}\phi_\theta - 3\sin2\phi\cos2\phi\psi_{\xi\xi\theta} \\
&- \sin2\phi\cos2\phi\psi_{\xi\xi}\phi_{\xi\xi} - 8\sin2\phi\cos2\phi\psi_{\xi\xi}\phi_\xi\phi_\theta + 6\sin2\phi\cos2\phi\psi_{\xi\xi}\phi_\xi \\
&+ \sin2\phi\cos2\phi\psi_{\xi\xi}\phi_{\theta\theta} + 2\sin2\phi\cos2\phi\psi_\xi\phi_{\xi\xi} + 3\sin2\phi\sin2\phi\psi_{\xi\theta\theta}\phi_\theta \\
&- \sin2\phi\sin2\phi\psi_{\xi\theta\theta} - \sin2\phi\sin2\phi\psi_{\xi\theta}\phi_{\xi\xi} - 8\sin2\phi\sin2\phi\psi_{\xi\theta}\phi_\xi\phi_\theta \\
&+ 6\sin2\phi\sin2\phi\psi_{\xi\theta}\phi_\xi + \sin2\phi\sin2\phi\psi_{\xi\theta}\phi_{\theta\theta} - 1/4\sin2\phi\sin2\phi\psi_{\xi\xi\xi\xi} \\
&- \sin2\phi\sin2\phi\psi_{\xi\xi\xi}\phi_\theta + \sin2\phi\sin2\phi\psi_{\xi\xi\xi} + 1/2\sin2\phi\sin2\phi\psi_{\xi\xi\theta\theta} \\
&- 3\sin2\phi\sin2\phi\psi_{\xi\xi\theta}\phi_\xi - \sin2\phi\sin2\phi\psi_{\xi\xi}\phi_{\xi\theta} + 2\sin2\phi\sin2\phi\psi_{\xi\xi}\phi_\xi^2 \\
&- 2\sin2\phi\sin2\phi\psi_{\xi\xi}\phi_\theta^2 + 3\sin2\phi\sin2\phi\psi_{\xi\xi}\phi_\theta - \sin2\phi\sin2\phi\psi_{\xi\xi} \\
&+ 2\sin2\phi\sin2\phi\psi_\xi\phi_{\xi\theta} - 4\sin2\phi\sin2\phi\psi_\xi\phi_\xi^2 + 4\sin2\phi\sin2\phi\psi_\xi\phi_\theta^2 \\
&- 2\sin2\phi\sin2\phi\psi_\xi\phi_\theta - 1/4\sin2\phi\sin2\phi\psi_{\theta\theta\theta\theta} + \sin2\phi\sin2\phi\psi_{\theta\theta\theta}\phi_\xi \\
&+ \sin2\phi\sin2\phi\psi_{\theta\theta}\phi_{\xi\theta} - 2\sin2\phi\sin2\phi\psi_{\theta\theta}\phi_\xi^2) + \alpha_2(\cos2\phi\psi_{\theta\theta}\phi_\theta^2
\end{aligned}
$$

$$
\begin{aligned}
&- \cos2\phi\psi_{\theta\theta}\phi_\theta - 1/2\cos2\phi\psi_\theta\phi_{\xi\theta\theta} + 4\cos2\phi\psi_\theta\phi_{\xi\theta}\phi_\xi + 1/2\cos2\phi\psi_\theta\phi_{\xi\xi\xi} \\
&+ 2\cos2\phi\psi_\theta\phi_{\xi\xi}\phi_\theta - \cos2\phi\psi_\theta\phi_{\xi\xi} - 2\cos2\phi\psi_\theta\phi_\xi^3 + 2\cos2\phi\psi_\theta\phi_\xi\phi_\theta^2 \\
&- 2\cos2\phi\psi_\theta\phi_\xi\phi_\theta - 1/2\psi_{\xi\theta\theta}\phi_\theta - 3/2\psi_{\xi\theta\theta} + \psi_{\xi\theta}\phi_{\xi\xi} - 2\psi_{\xi\theta}\phi_\xi - \psi_{\xi\theta}\phi_{\theta\theta} \\
&+ 1/4\psi_{\xi\xi\xi\xi} - 1/2\psi_{\xi\xi\xi}\phi_\theta - 3/2\psi_{\xi\xi\xi} + 1/2\psi_{\xi\xi\theta\theta} + 1/2\psi_{\xi\xi\theta}\phi_\xi - \psi_{\xi\xi}\phi_{\xi\theta} \\
&+ 2\psi_{\xi\xi}\phi_\theta + 3\psi_{\xi\xi} + 2\psi_\xi\phi_{\xi\theta} - 1/2\psi_\xi\phi_{\xi\xi\theta} - 1/2\psi_\xi\phi_{\theta\theta\theta} - 2\psi_\xi\phi_\theta - 2\psi_\xi \\
&+ 1/4\psi_{\theta\theta\theta\theta} + 1/2\psi_{\theta\theta\theta}\phi_\xi + \psi_{\theta\theta}\phi_{\xi\theta} + \psi_{\theta\theta} + 1/2\psi_\theta\phi_{\xi\theta\theta} + 1/2\psi_\theta\phi_{\xi\xi\xi} - 2\psi_\theta\phi_{\xi\xi} \\
&+ 2\psi_\theta\phi_\xi - 4\sin2\phi\psi_\theta\phi_\xi^2\phi_\theta + 2\sin2\phi\psi_\theta\phi_\xi^2 + \sin2\phi\psi_\theta\phi_\xi\phi_{\theta\theta} + 3/2\cos2\phi\psi_{\xi\theta\theta}\phi_\theta \\
&+ \cos2\phi\psi_{\xi\theta}\phi_{\xi\xi} - 3\cos2\phi\psi_{\xi\theta}\phi_\xi + \cos2\phi\psi_{\xi\theta}\phi_{\theta\theta} + 1/4\cos2\phi\psi_{\xi\xi\xi\xi} \\
&+ 1/2\cos2\phi\psi_{\xi\xi\xi}\phi_\theta - \cos2\phi\psi_{\xi\xi\xi} + 3/2\cos2\phi\psi_{\xi\xi\theta}\phi_\xi - \cos2\phi\psi_{\xi\xi}\phi_\xi^2 \\
&- \cos2\phi\psi_{\xi\xi}\phi_\theta^2 - 2\cos2\phi\psi_{\xi\xi}\phi_\theta + \cos2\phi\psi_{\xi\xi} - 4\cos2\phi\psi_\xi\phi_{\xi\theta}\phi_\theta - \cos2\phi\psi_\xi\phi_{\xi\theta} \\
&- 1/2\cos2\phi\psi_\xi\phi_{\xi\xi\theta} + 2\cos2\phi\psi_\xi\phi_\xi^2\phi_\theta + 2\cos2\phi\psi_\xi\phi_\xi^2 - 2\cos2\phi\psi_\xi\phi_\xi\phi_{\theta\theta} \\
&+ 1/2\cos2\phi\psi_\xi\phi_{\theta\theta\theta} - 2\cos2\phi\psi_\xi\phi_\theta^3 + 2\cos2\phi\psi_\xi\phi_\theta - 1/4\cos2\phi\psi_{\theta\theta\theta\theta} \\
&+ 1/2\cos2\phi\psi_{\theta\theta\theta}\phi_\xi + \cos2\phi\psi_{\theta\theta}\phi_\xi^2 + 1/2\sin2\phi\psi_{\xi\theta\theta\theta} - 2\sin2\phi\psi_{\xi\theta}\phi_\xi^2 \\
&- 2\sin2\phi\psi_{\xi\theta}\phi_\theta^2 - \sin2\phi\psi_{\xi\theta}\phi_\theta + \sin2\phi\psi_{\xi\theta} + 1/2\sin2\phi\psi_{\xi\xi\xi\theta} - \sin2\phi\psi_{\xi\xi\xi}\phi_\xi \\
&- 3/2\sin2\phi\psi_{\xi\xi\theta} - 1/2\sin2\phi\psi_{\xi\xi}\phi_{\xi\xi} + 3\sin2\phi\psi_{\xi\xi}\phi_\xi - 1/2\sin2\phi\psi_{\xi\xi}\phi_{\theta\theta} \\
&- \sin2\phi\psi_\xi\phi_{\xi\theta\theta} + 2\sin2\phi\psi_\xi\phi_{\xi\theta}\phi_\xi + \sin2\phi\psi_\xi\phi_{\xi\xi}\phi_\theta + \sin2\phi\psi_\xi\phi_{\xi\xi} \\
&+ 4\sin2\phi\psi_\xi\phi_\xi\phi_\theta^2 + 2\sin2\phi\psi_\xi\phi_\xi\phi_\theta - 2\sin2\phi\psi_\xi\phi_\xi - 3\sin2\phi\psi_\xi\phi_{\theta\theta}\phi_\theta \\
&+ \sin2\phi\psi_{\theta\theta\theta}\phi_\theta - 1/2\sin2\phi\psi_{\theta\theta\theta} + 1/2\sin2\phi\psi_{\theta\theta}\phi_{\xi\xi} + 1/2\sin2\phi\psi_{\theta\theta}\phi_{\theta\theta} \\
&+ 2\sin2\phi\psi_\theta\phi_{\xi\theta}\phi_\theta - \sin2\phi\psi_\theta\phi_{\xi\theta} + \sin2\phi\psi_\theta\phi_{\xi\xi\theta} - 3\sin2\phi\psi_\theta\phi_{\xi\xi}\phi_\xi) \\
&+ \alpha_3(\cos2\phi\psi_{\theta\theta}\phi_\theta^2 - \cos2\phi\psi_{\theta\theta}\phi_\theta - 1/2\cos2\phi\psi_\theta\phi_{\xi\theta\theta} + 4\cos2\phi\psi_\theta\phi_{\xi\theta}\phi_\xi \\
&+ 1/2\cos2\phi\psi_\theta\phi_{\xi\xi\xi} + 2\cos2\phi\psi_\theta\phi_{\xi\xi}\phi_\theta - \cos2\phi\psi_\theta\phi_{\xi\xi} - 2\cos2\phi\psi_\theta\phi_\xi^3 \\
&+ 2\cos2\phi\psi_\theta\phi_\xi\phi_\theta^2 - 2\cos2\phi\psi_\theta\phi_\xi\phi_\theta + 1/2\psi_{\xi\theta\theta}\phi_\theta + 3/2\psi_{\xi\theta\theta} - \psi_{\xi\theta}\phi_{\xi\xi} + 2\psi_{\xi\theta}\phi_\xi \\
&+ \psi_{\xi\theta}\phi_{\theta\theta} - 1/4\psi_{\xi\xi\xi\xi} + 1/2\psi_{\xi\xi\xi}\phi_\theta + 3/2\psi_{\xi\xi\xi} - 1/2\psi_{\xi\xi\theta\theta} - 1/2\psi_{\xi\xi\theta}\phi_\xi + \psi_{\xi\xi}\phi_{\xi\theta} \\
&- 2\psi_{\xi\xi}\phi_\theta - 3\psi_{\xi\xi} - 2\psi_\xi\phi_{\xi\theta} + 1/2\psi_\xi\phi_{\xi\xi\theta} + 1/2\psi_\xi\phi_{\theta\theta\theta} + 2\psi_\xi\phi_\theta + 2\psi_\xi \\
&- 1/4\psi_{\theta\theta\theta\theta} - 1/2\psi_{\theta\theta\theta}\phi_\xi - \psi_{\theta\theta}\phi_{\xi\theta} - \psi_{\theta\theta} - 1/2\psi_\theta\phi_{\xi\theta\theta} - 1/2\psi_\theta\phi_{\xi\xi\xi} \\
&+ 2\psi_\theta\phi_{\xi\xi} - 2\psi_\theta\phi_\xi - 4\sin2\phi\psi_\theta\phi_\xi^2\phi_\theta + 2\sin2\phi\psi_\theta\phi_\xi^2 + \sin2\phi\psi_\theta\phi_\xi\phi_{\theta\theta} \\
&+ 3/2\cos2\phi\psi_{\xi\theta\theta}\phi_\theta + \cos2\phi\psi_{\xi\theta}\phi_{\xi\xi} - 3\cos2\phi\psi_{\xi\theta}\phi_\xi + \cos2\phi\psi_{\xi\theta}\phi_{\theta\theta} \\
&+ 1/4\cos2\phi\psi_{\xi\xi\xi\xi} + 1/2\cos2\phi\psi_{\xi\xi\xi}\phi_\theta - \cos2\phi\psi_{\xi\xi\xi} + 3/2\cos2\phi\psi_{\xi\xi\theta}\phi_\xi \\
&- \cos2\phi\psi_{\xi\xi}\phi_\xi^2 - \cos2\phi\psi_{\xi\xi}\phi_\theta^2 - 2\cos2\phi\psi_{\xi\xi}\phi_\theta + \cos2\phi\psi_{\xi\xi} - 4\cos2\phi\psi_\xi\phi_{\xi\theta}\phi_\theta \\
&- \cos2\phi\psi_\xi\phi_{\xi\theta} - 1/2\cos2\phi\psi_\xi\phi_{\xi\xi\theta} + 2\cos2\phi\psi_\xi\phi_\xi^2\phi_\theta + 2\cos2\phi\psi_\xi\phi_\xi^2 \\
&- 2\cos2\phi\psi_\xi\phi_\xi\phi_{\theta\theta} + 1/2\cos2\phi\psi_\xi\phi_{\theta\theta\theta} - 2\cos2\phi\psi_\xi\phi_\theta^3 + 2\cos2\phi\psi_\xi\phi_\theta
\end{aligned}
$$

$$
\begin{aligned}
&- 1/4\cos 2\phi\psi_{\theta\theta\theta\theta} + 1/2\cos 2\phi\psi_{\theta\theta\theta}\phi_\xi + \cos 2\phi\psi_{\theta\theta}\phi_\xi^2 + 1/2\sin 2\phi\psi_{\xi\theta\theta\theta} \\
&- 2\sin 2\phi\psi_{\xi\theta}\phi_\xi^2 - 2\sin 2\phi\psi_{\xi\theta}\phi_\theta^2 - \sin 2\phi\psi_{\xi\theta}\phi_\theta + \sin 2\phi\psi_{\xi\theta} + 1/2\sin 2\phi\psi_{\xi\xi\xi\theta} \\
&- \sin 2\phi\psi_{\xi\xi\xi}\phi_\xi - 3/2\sin 2\phi\psi_{\xi\xi\theta} - 1/2\sin 2\phi\psi_{\xi\xi}\phi_{\xi\xi} + 3\sin 2\phi\psi_{\xi\xi}\phi_\xi \\
&- 1/2\sin 2\phi\psi_{\xi\xi}\phi_{\theta\theta} - \sin 2\phi\psi_\xi\phi_{\xi\theta\theta} + 2\sin 2\phi\psi_\xi\phi_{\xi\theta}\phi_\xi + \sin 2\phi\psi_\xi\phi_{\xi\xi}\phi_\theta \\
&+ \sin 2\phi\psi_\xi\phi_{\xi\xi} + 4\sin 2\phi\psi_\xi\phi_\xi\phi_\theta^2 + 2\sin 2\phi\psi_\xi\phi_\xi\phi_\theta - 2\sin 2\phi\psi_\xi\phi_\xi \\
&- 3\sin 2\phi\psi_\xi\phi_{\theta\theta}\phi_\theta + \sin 2\phi\psi_{\theta\theta\theta}\phi_\theta - 1/2\sin 2\phi\psi_{\theta\theta\theta} + 1/2\sin 2\phi\psi_{\theta\theta}\phi_{\xi\xi} \\
&+ 1/2\sin 2\phi\psi_{\theta\theta}\phi_{\theta\theta} + 2\sin 2\phi\psi_\theta\phi_{\xi\theta}\phi_\theta - \sin 2\phi\psi_\theta\phi_{\xi\theta} + \sin 2\phi\psi_\theta\phi_{\xi\xi\theta} \\
&- 3\sin 2\phi\psi_\theta\phi_{\xi\xi}\phi_\xi) + \alpha_5(-\cos 2\phi\psi_{\xi\theta}\phi_{\theta\theta} - 1/4\cos 2\phi\psi_{\xi\xi\xi\xi} + 3/2\cos 2\phi\psi_{\xi\xi\xi} \\
&- 2\cos 2\phi\psi_{\xi\xi\theta}\phi_\xi + \cos 2\phi\psi_{\xi\xi}\phi_\xi^2 + \cos 2\phi\psi_{\xi\xi}\phi_\theta^2 - 3\cos 2\phi\psi_{\xi\xi} - 2\cos 2\phi\psi_\xi\phi_\xi^2 \\
&- 2\cos 2\phi\psi_\xi\phi_\theta^2 + 2\cos 2\phi\psi_\xi + 1/4\cos 2\phi\psi_{\theta\theta\theta\theta} - \cos 2\phi\psi_{\theta\theta}\phi_\xi^2 - \cos 2\phi\psi_{\theta\theta}\phi_\theta^2 \\
&+ 2\cos 2\phi\psi_{\theta\theta}\phi_\theta + \cos 2\phi\psi_{\theta\theta} + \cos 2\phi\psi_\theta\phi_{\xi\xi} - 4\cos 2\phi\psi_\theta\phi_\xi + \cos 2\phi\psi_\theta\phi_{\theta\theta} \\
&+ \psi_{\xi\theta} - 1/4\psi_{\xi\xi\xi\xi} + \psi_{\xi\xi\xi} - 1/2\psi_{\xi\xi\theta\theta} - \psi_{\xi\xi} - 1/4\psi_{\theta\theta\theta\theta} - \psi_{\theta\theta} - 1/2\sin 2\phi\psi_{\xi\theta\theta\theta} \\
&- \sin 2\phi\psi_{\xi\theta\theta}\phi_\xi + 2\sin 2\phi\psi_{\xi\theta}\phi_\xi^2 + 2\sin 2\phi\psi_{\xi\theta}\phi_\theta^2 - 2\sin 2\phi\psi_{\xi\theta}\phi_\theta - 4\sin 2\phi\psi_{\xi\theta} \\
&- 1/2\sin 2\phi\psi_{\xi\xi\xi\theta} + \sin 2\phi\psi_{\xi\xi\xi}\phi_\xi + \sin 2\phi\psi_{\xi\xi\theta}\phi_\theta + 5/2\sin 2\phi\psi_{\xi\xi\theta} \\
&+ 1/2\sin 2\phi\psi_{\xi\xi}\phi_{\xi\xi} - 4\sin 2\phi\psi_{\xi\xi}\phi_\xi + 1/2\sin 2\phi\psi_{\xi\xi}\phi_{\theta\theta} - \sin 2\phi\psi_\xi\phi_{\xi\xi} \\
&+ 4\sin 2\phi\psi_\xi\phi_\xi - \sin 2\phi\psi_\xi\phi_{\theta\theta} - \sin 2\phi\psi_{\theta\theta\theta}\phi_\theta + 1/2\sin 2\phi\psi_{\theta\theta\theta} - 1/2\sin 2\phi\psi_{\theta\theta}\phi_{\xi\xi} \\
&+ 2\sin 2\phi\psi_{\theta\theta}\phi_\xi - 1/2\sin 2\phi\psi_{\theta\theta}\phi_{\theta\theta} - 2\sin 2\phi\psi_\theta\phi_\xi^2 - 2\sin 2\phi\psi_\theta\phi_\theta^2 + 2\sin 2\phi\psi_\theta \\
&- 2\cos 2\phi\psi_{\xi\theta\theta}\phi_\theta - 1/2\cos 2\phi\psi_{\xi\theta\theta} - \cos 2\phi\psi_{\xi\theta}\phi_{\xi\xi} + 6\cos 2\phi\psi_{\xi\theta}\phi_\xi) \\
&+ \alpha_6(1/4\cos 2\phi\psi_{\xi\xi\xi\xi} - 3/2\cos 2\phi\psi_{\xi\xi\xi} + 2\cos 2\phi\psi_{\xi\xi\theta}\phi_\xi - \cos 2\phi\psi_{\xi\xi}\phi_\xi^2 \\
&- \cos 2\phi\psi_{\xi\xi}\phi_\theta^2 + 3\cos 2\phi\psi_{\xi\xi} + 2\cos 2\phi\psi_\xi\phi_\xi^2 + 2\cos 2\phi\psi_\xi\phi_\theta^2 - 2\cos 2\phi\psi_\xi \\
&- 1/4\cos 2\phi\psi_{\theta\theta\theta\theta} + \cos 2\phi\psi_{\theta\theta}\phi_\xi^2 + \cos 2\phi\psi_{\theta\theta}\phi_\theta^2 - 2\cos 2\phi\psi_{\theta\theta}\phi_\theta - \cos 2\phi\psi_{\theta\theta} \\
&- \cos 2\phi\psi_\theta\phi_{\xi\xi} + 4\cos 2\phi\psi_\theta\phi_\xi - \cos 2\phi\psi_\theta\phi_{\theta\theta} + \psi_{\xi\theta\theta} - 1/4\psi_{\xi\xi\xi\xi} + \psi_{\xi\xi\xi} \\
&- 1/2\psi_{\xi\xi\theta\theta} - \psi_{\xi\xi} - 1/4\psi_{\theta\theta\theta\theta} - \psi_{\theta\theta} + 1/2\sin 2\phi\psi_{\xi\theta\theta\theta} + \sin 2\phi\psi_{\xi\theta\theta}\phi_\xi \\
&- 2\sin 2\phi\psi_{\xi\theta}\phi_\xi^2 - 2\sin 2\phi\psi_{\xi\theta}\phi_\theta^2 + 2\sin 2\phi\psi_{\xi\theta}\phi_\theta + 4\sin 2\phi\psi_{\xi\theta} + 1/2\sin 2\phi\psi_{\xi\xi\xi\theta} \\
&- \sin 2\phi\psi_{\xi\xi\xi}\phi_\xi - \sin 2\phi\psi_{\xi\xi\theta}\phi_\theta - 5/2\sin 2\phi\psi_{\xi\xi\theta} - 1/2\sin 2\phi\psi_{\xi\xi}\phi_{\xi\xi} \\
&+ 4\sin 2\phi\psi_{\xi\xi}\phi_\xi - 1/2\sin 2\phi\psi_{\xi\xi}\phi_{\theta\theta} + \sin 2\phi\psi_\xi\phi_{\xi\xi} - 4\sin 2\phi\psi_\xi\phi_\xi + \sin 2\phi\psi_\xi\phi_{\theta\theta} \\
&+ \sin 2\phi\psi_{\theta\theta\theta}\phi_\theta - 1/2\sin 2\phi\psi_{\theta\theta\theta} + 1/2\sin 2\phi\psi_{\theta\theta}\phi_{\xi\xi} - 2\sin 2\phi\psi_{\theta\theta}\phi_\xi \\
&+ 1/2\sin 2\phi\psi_{\theta\theta}\phi_{\theta\theta} + 2\sin 2\phi\psi_\theta\phi_\xi^2 + 2\sin 2\phi\psi_\theta\phi_\theta^2 - 2\sin 2\phi\psi_\theta + 2\cos 2\phi\psi_{\xi\theta\theta}\phi_\theta \\
&+ 1/2\cos 2\phi\psi_{\xi\theta\theta} + \cos 2\phi\psi_{\xi\theta}\phi_{\xi\xi} - 6\cos 2\phi\psi_{\xi\theta}\phi_\xi + \cos 2\phi\psi_{\xi\theta}\phi_{\theta\theta})
\end{aligned}
$$